China Geology 9 (2026) 553−566

China Geology

Journal homepage: http://chinageology.cgs.cn
https://www.sciencedirect.com/journal/china-geology

# A thermoresponsive temporary plugging agent for drilling fluids in marine gas hydrate reservoirs: Synthesis, performance, and reversible plugging mechanism

Jin-tang Wang[a, b], Ke Zhao[a, b], Bo Liao[a, b,*], Lei Liu[c], Kai-he Lü[a, b], Jin-sheng Sun[a, b], Shu-qiang Shi[d]

[a] *School of Petroleum Engineering*, *China University of Petroleum* (*East China*), *Qingdao* 266580, *China*
[b] *Key Laboratory of Unconventional Oil & Gas Development*, *Ministry of Education*, *Qingdao* 266580, *China*
[c] *PetroChina Coalbed Methane Company Limited*, *Beijing* 100028, *China*
[d] *School of Petroleum Engineering*, *Chongqing University of Science and Technology*, *Chongqing* 401331, *China*

A R T I C L E  I N F O

*Article history:*
Received 12 June 2025
Received in revised form 19 November 2025
Accepted 8 January 2026
Available online 25 February 2026

*Keywords:*
Natural gas hydrates
Combustible ice
Clean energy
Unconventional energy
Gas hydrate reservoir
Water-based drilling fluids
Thermoresponsive polymers
Temporary plugging agent
Mechanism analysis
Low-field nuclear magnetic resonance imaging
Lower critical solution temperature

A B S T R A C T

During drilling in marine gas hydrate reservoirs, drilling-fluid invasion can induce hydrate dissociation, wellbore instability, and reservoir damage, thereby compromising drilling safety and reservoir protection. To address the low-temperature agglomeration and limited self-unplugging capability of conventional temporary plugging agents, a water-soluble thermoresponsive temporary plugging agent (TRP) was synthesized via free-radical copolymerization. Its structural characteristics, phase-transition behavior, plugging performance, reversible unplugging capacity, and underlying mechanism were systematically investigated through laboratory experiments and low-field nuclear magnetic resonance (NMR) imaging. The results show that TRP exhibits a lower critical solution temperature (LCST) of approximately 15°C, matching the thermal conditions of marine hydrate reservoirs. Above the LCST, TRP rapidly aggregates to form a dense plugging layer, effectively suppressing drilling-fluid invasion; below the LCST, it redissolves and restores formation permeability, with a maximum permeability recovery of 96.8%. Sand-disk filtration tests further demonstrate that TRP provides more effective fluid-loss control than ultrafine $CaCO_3$ and nano-emulsion under the tested conditions. Low-field NMR imaging directly visualizes the invasion–plugging–unplugging process. Mechanism analysis indicates that plugging originates from hydrophobic association of polymer chains above the LCST, which enhances filter cake compactness and increases the rock-surface contact angle from 41.5° to 77.4°. This reversible thermoresponsive strategy provides a practical basis for intelligent reservoir protection during deep-sea hydrate drilling.

©2026 China Geology Editorial Office.

## 1. Introduction

With the gradual depletion of conventional fossil energy resources and increasing pressure on ecological environments, the development of new, efficient, and clean energy sources has become an inevitable choice for the global energy transition (Mu LF et al., 2025). Natural gas hydrates are ice-like clathrate crystalline substances formed by the combination of water molecules and natural gas molecules under low-temperature and high-pressure conditions. They are abundant in submarine sediments and onshore permafrost zones (Liao B et al., 2022). Notably, marine gas hydrate resources account for approximately 97% of the global total, with their calorific value estimated to be about twice that of the world's proven reserves of coal, petroleum, and natural gas combined (Sun JS et al., 2021; Qin XW et al., 2022; Su PB et al., 2024). Compared to traditional fossil fuels, natural gas hydrates offer significant advantages in terms of environmental friendliness and abundance (Zhu YH et al., 2021). As a result, they are considered an ideal alternative energy source during the carbon-neutral transition period and have attracted considerable global attention (Wang XC et al., 2023). Drilling serves as the sole pathway connecting the surface to deep-sea natural gas hydrate reservoirs and represents a core operation in petroleum engineering (Yang J et al., 2023). As an essential component of drilling operations, drilling fluids play critical roles in maintaining formation pressure balance, acquiring formation information, stabilizing the wellbore, and protecting the reservoir (Wang JT et al.,

First author: *E-mail address*: wangjintang@upc.edu.cn (Jin-tang Wang).

* Corresponding author: *E-mail address*: liaobo@outlook.com (Bo Liao).

Literary editor: Xi-jie Chen
doi:10.31035/cg2025145
2096-5192/© 2026 China Geology Editorial Office.

Copyright © 2026 Editorial Office of China Geology. Publishing services by Elsevier B.V. on behalf of KeAi Communications Co. Ltd.
This is an open access article under the CC BY-NC-ND License (http://creativecommons.org/licenses/by-nc-nd/4.0/).

2024a). Drilling in deep-sea, low-temperature natural gas hydrate reservoirs is typically performed under a positive pressure differential (Liao YQ et al., 2021). Under these conditions, drilling fluids tend to invade the reservoir through heat transfer and fluid flow, thereby inducing the decomposition of gas hydrates. This process reduces the effective stress and cementation strength of the formation, leading to wellbore instability and reservoir damage (Huang TJ et al., 2020; Zhao K et al., 2024). The addition of appropriate plugging agents to drilling fluids can effectively reduce fluid invasion and minimize disturbance to hydrate-bearing formations (Wang R et al., 2023). Currently, commonly used plugging agents in deepwater drilling fluids include materials such as ultrafine calcium carbonate and sulfonated asphalt (Wang R et al., 2019; Wang JT et al., 2024b). However, several prominent issues remain in practical applications: (1) Owing to their extensive specific surface area and elevated surface free energy, they are prone to agglomeration at low temperatures, thus reducing their plugging efficiency for microfractures; (2) these materials are difficult to degrade, and conventional removal operations may cause secondary damage to the hydrate reservoir, further reducing its permeability and compromising the effectiveness of reservoir protection (Ye L et al., 2020).

To enhance the overall performance of drilling fluids, temporary plugging agents with controllable plugging and removal capabilities have become crucial for improving drilling safety and protecting the reservoir. Current research is primarily focused on the development of temporary plugging agents for drilling fluids that offer controllable plugging and self-removal properties. The design and development of such materials require them to exhibit effective plugging and self-degradation performance across diverse reservoir environments (Sun JS et al., 2024). According to different removal mechanisms, temporary plugging agents can be classified into four categories: Water-soluble, oil-soluble, acid-soluble, and alkali-soluble materials, in order to meet the varied demands of drilling under different formation conditions (Wei AC et al., 2023; Wu GA et al., 2023; Dong XQ et al., 2024). However, in marine gas hydrate reservoirs, conventional materials often become unstable at low temperatures or lack sufficient strength under high pressure, making it difficult to adapt to changing reservoir environments. Additionally, due to the poor cementation of hydrate-bearing formations, acid-soluble and alkali-soluble materials also face certain limitations during the plug removal process (Niu C et al., 2024). Therefore, the development of water-soluble thermoresponsive temporary plugging agents has become essential for addressing these challenges.

The main characteristic of thermoresponsive temporary plugging agents is their ability to modulate their physicochemical properties, such as solubility, viscosity, and gel strength, in response to temperature changes, thereby enabling solidification for effective plugging. Under specific temperature conditions, these materials can undergo self-removal, effectively restoring reservoir permeability (Li X et al., 2023). The phase transition mechanism of thermoresponsive polymers is based on the coexistence of hydrophilic and hydrophobic groups within their molecular chains. The interaction of hydrophilic and hydrophobic groups with water changes depending on temperature, resulting in the thermoresponsive polymer solution transitioning from a clear, uniform state to an opaque solid-liquid dispersion when a specific temperature is reached; this temperature is referred to as the phase transition point of the polymer (Hsu SH and Yu TL, 2000; Suleimenov I et al., 2017). When the temperature exceeds the LCST, the polymer spontaneously separates and aggregates, forming effective plugging structures in the reservoir. Conversely, when the temperature drops below the LCST, the polymer re-disperses and dissolves, thereby removing the plugging layer and restoring reservoir permeability. Currently, LCST-type thermoresponsive polymers have been extensively studied, with a variety of chemical structures available. These include polyacrylamides, polyethers, polyvinylamides, polymethacrylates, and polyoxazolines (Wang LS et al., 2006; Zarrintaj P et al., 2019; Liu C et al., 2021). Water-soluble LCST-type thermoresponsive temporary plugging agents designed for drilling fluids in marine gas hydrate reservoirs can effectively reduce the invasion of drilling fluids into the reservoir. Moreover, during depressurization-based hydrate production, these polymers can re-dissolve as the reservoir temperature decreases, restoring reservoir permeability and thus minimizing reservoir damage.

Therefore, in this study, a novel water-soluble thermoresponsive temporary plugging agent (TRP) suitable for deep-sea, low-temperature marine gas hydrate reservoirs was developed by employing the thermoresponsive polymer monomer N-isopropylacrylamide (NIPAM), taking into account the unique characteristics of such reservoirs. Through an in-depth investigation of the performance and adaptability of the thermoresponsive plugging agent under complex shallow geological conditions in deepwater environments, this work aims to overcome the limitations of conventional plugging agents. Moreover, an experimental approach based on low-field nuclear magnetic resonance (NMR) analysis was developed to evaluate the temporary plugging performance. The underlying plugging mechanisms of the new agent were elucidated, offering valuable theoretical insights and technological support for ensuring the secure and efficient development of natural gas hydrate resources.

## 2. Materials and methods

### *2.1. Materials*

The chemicals required for the synthesis experiment of thermoresponsive temporary plugging agents (TRP) for drilling fluids in hydrate reservoirs are listed in Table 1.

### *2.2. Preparation of the TRP*

A mixture of NIPAM (12.93 g), BMA (1.81 g), and AMPS (0.26 g) with a molar ratio of 90∶10∶1 was added to a three-neck flask. Subsequently, 85 mL of DMF was

introduced as the solvent. Nitrogen gas was bubbled through the solution in the flask to remove dissolved oxygen. The reaction system was then placed in a 40°C water bath with continuous mechanical stirring to fully dissolve the monomers, while nitrogen purging was maintained for 40 minutes to ensure complete deoxygenation. After the temperature of the water bath was raised to 65°C and maintained for 10 minutes, a solution of AIBN (0.015 g, corresponding to 0.1% of the total solids) in DMF was slowly added via a constant-pressure dropping funnel. The polymerization was carried out at 65°C in a nitrogen environment for a duration of 8 hours.

Upon completion of the reaction, the product was poured into an excess of ultrapure water at 40°C and stirred for 10 minutes to facilitate the precipitation of the polymer. The resulting suspension was then transferred to a Büchner funnel for vacuum filtration, and the precipitate was washed with anhydrous ethanol to remove impurities. The sample was ultimately transferred to a vacuum oven set at 60°C and subjected to vacuum drying for 48 hours. The resulting material was the TRP suitable for drilling fluids in deep-sea, low-temperature natural gas hydrate reservoirs. The specific synthetic route is illustrated in Fig. 1.

### 2.3. Structural characterization of TRP

#### 2.3.1. Infrared spectral analysis

The molecular structure of TRP was characterized utilizing a Fourier transform infrared (FTIR) spectrometer (IRTracer-100, Shimadzu, Japan). After vacuum drying, the sample was finely ground and blended with potassium bromide (KBr) at a mass ratio of 1∶100. The homogeneous mixture was pressed into pellets. FTIR spectra of the copolymer were collected across the 400–4000 $cm^{-1}$ region. The obtained spectra were subsequently interpreted to verify the molecular structure information of the synthesized products.

#### 2.3.2. UV-Visible spectroscopy analysis

The thermoresponsive properties of TRP were evaluated using a UV-Visible spectrophotometer (model UV 3100 PC, Shanghai Mapada Instruments Co., Ltd.). The synthesized TRP was dissolved in ultrapure water at a concentration of 2%, and the transmittance of the polymer solution was monitored at a wavelength of 600 nm over a temperature range of 10°C–30°C. During the heating process, the transmittance was measured in real time. The temperature at which the transmittance decreased to 50% of its initial value

**Table 1. Experimental materials.**

| Material | Specification | Supplier |
|---|---|---|
| Isopropylacrylamide (NIPAM) | Chemically pure | Shanghai McLean Biochemical Technology Co., Ltd. |
| Butyl methacrylate (BMA) | Chemically pure | Shanghai McLean Biochemical Technology Co., Ltd. |
| 2-acrylamido-2-methylpropane sulfonic acid (AMPS) | Chemically pure | Shanghai Aladdin Biochemical Technology Co., Ltd. |
| N,N-dimethylformamide (DMF) | Chemically pure | Shanghai Aladdin Biochemical Technology Co., Ltd. |
| Azodiisobutyronitrile (AIBN) | Chemically pure | Chemical Reagent Co., Ltd. |
| Absolute alcohol | Chemically pure | Shanghai Aladdin Biochemical Technology Co., Ltd. |
| Pure water | Resistivity ≥ 18.2 MΩ·cm (25°C) | Laboratory-made |

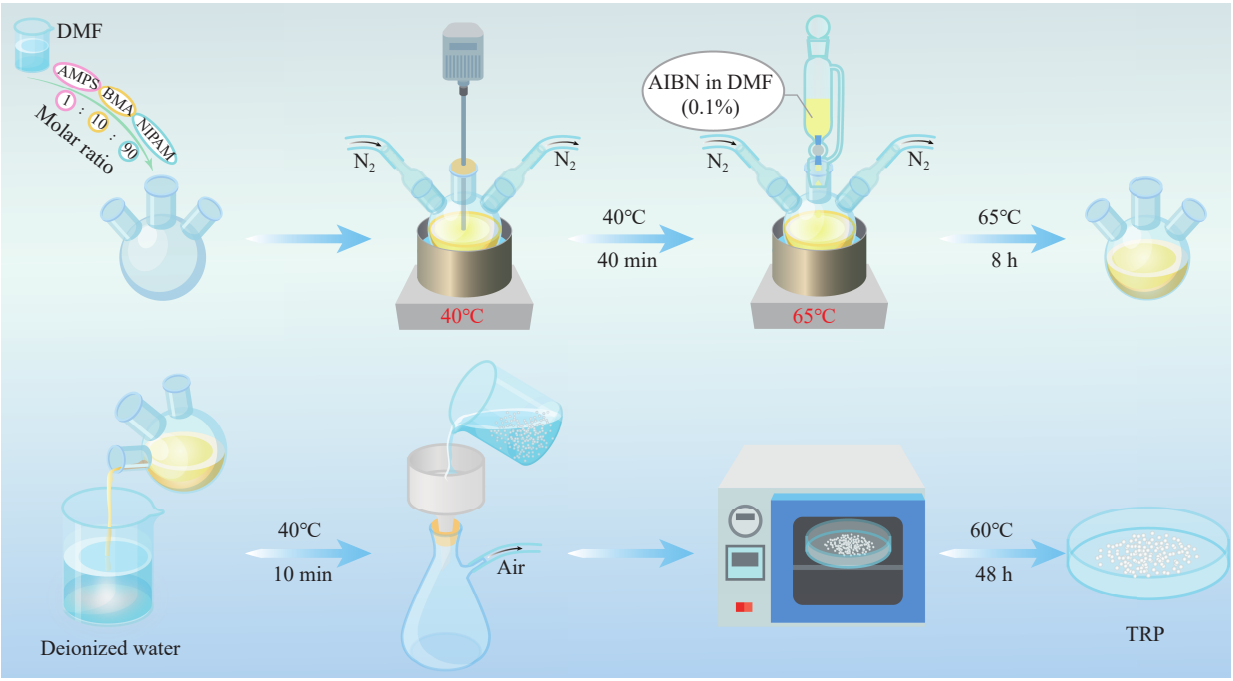


**Fig. 1.** Schematic diagram of the synthetic route for the thermoresponsive temporary plugging agent (TRP).

was defined as the LCST of the thermoresponsive polymer (Lou SF et al., 2013; Kubo M et al., 2021).

*2.3.3. Particle size distribution and zeta potential analysis*

TRP particle size distribution in aqueous solution was evaluated employing a nanoparticle size and zeta potential analyzer (Zetasizer Nano Z, Malvern Instruments, UK) with a sample concentration of 0.05 mg/mL. Measurements were carried out at 19°C to characterize particle size in the aqueous medium. The instrument also allowed simultaneous determination of the zeta potential for the TRP samples. A certain amount of TRP was added to a 4% bentonite slurry, and the mixture was diluted accordingly. The diluted solution was then transferred into a specialized sample cell for the zeta potential analyzer. By varying the dosage of TRP, the zeta potential values were measured to evaluate the dispersion and stability of TRP in the drilling fluid system.

*2.4. Performance evaluation of TRP*

To prepare the base drilling fluid slurry, 40 g of bentonite and 2.4 g of anhydrous sodium carbonate were incrementally added to 1000 mL of deionized water. The solution was stirred at 8000 rpm until uniformity was obtained, after which it was sealed and left to stand for 24 hours. Under continuous stirring at 6000 rpm, varying concentrations of TRP were gradually added to the base slurry to prepare mixtures containing TRP. The API fluid loss values of drilling fluid slurries with different TRP concentrations were measured for 30 minutes using a standard SD6A API filter press and a low-pressure, low-temperature (LPLT) API filter press (Fann Instrument Company) at a constant pressure of 0.7 MPa. These tests were conducted under both ambient and simulated deep-sea low-temperature conditions to evaluate the effect of TRP concentration on the filtration performance of the bentonite-based drilling fluid.

Considering the actual application environment of drilling fluids, a ceramic disk with an average pore size of 3 μm was used to simulate the pore-throat structure of hydrate-bearing sediments. To further assess the plugging performance of TRP, comparative experiments were performed using ultrafine calcium carbonate and nano-emulsion as reference plugging agents. Specifically, 2% TRP, 2% ultrafine calcium carbonate, and 2% nano-emulsion were each added to a 4% bentonite slurry. Sand disk plugging and permeability tests were conducted at a pressure of 3.5 MPa, and the filtration loss over 30 minutes was recorded to compare the plugging performance of the different agents.

*2.5. Evaluation of the temporary plugging performance of TRP in simulated hydrate reservoirs using low-field nuclear magnetic resonance (NMR)*

*2.5.1. Low-field nuclear magnetic resonance (NMR) technology*

To evaluate the temporary plugging performance of the TRP under these conditions, the NMR imaging analyzer (MacroMR12-150I) was modified in this study. A custom experimental setup was designed to enable dynamic monitoring of drilling fluid invasion into hydrate-bearing reservoirs. As depicted in Fig. 2, the setup is composed mainly of an NMR system, core displacement unit, temperature and pressure regulation modules, and a data collection subsystem (Shao ZH et al., 2023).

The NMR device operated at a magnetic field strength of 0.3 Tesla and a principal frequency of 12.0 MHz. Throughout the experiment, ambient temperature was controlled at 26 ± 0.5°C to maintain magnetic field stability. Low-field NMR technology characterizes the state of pore fluids by analyzing the relaxation rates of hydrogen protons in liquid water. Liquid water in different occurrence states exhibits significant differences in hydrogen proton relaxation rates. A faster relaxation rate indicates a higher degree of molecular confinement, while a slower rate suggests a more mobile water state (Yang MJ et al., 2017; Ge XM et al., 2018).

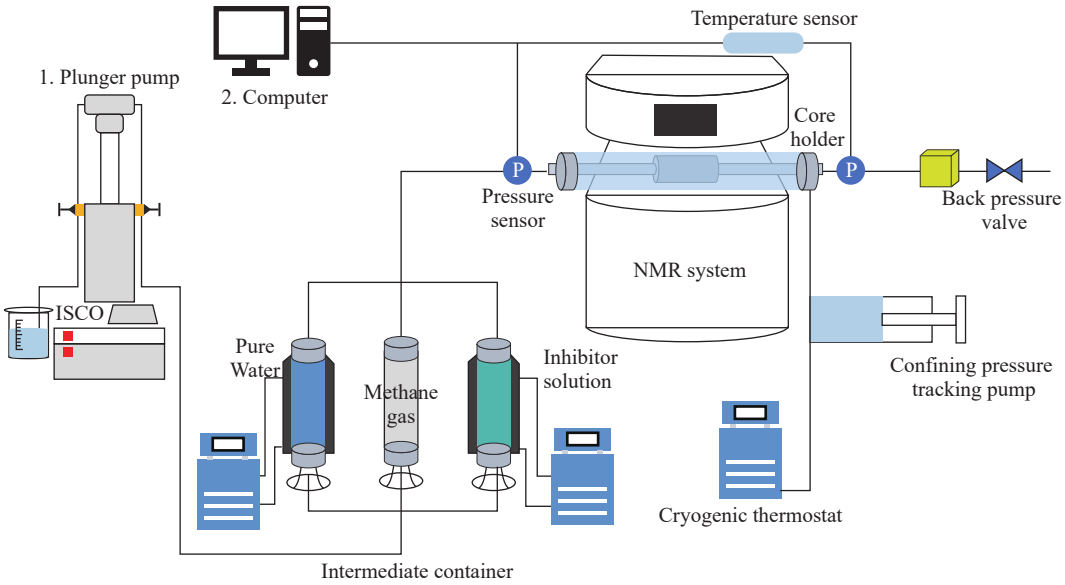


**Fig. 2.** Experimental apparatus for investigating fluid invasion into hydrate-bearing sediment (after Shao ZH et al., 2023).

Utilizing this concept in conjunction with magnetic resonance imaging (MRI) techniques enables non-destructive visualization of the spatial arrangement of water protons, thus allowing for quantitative assessment of pore water content.

The core displacement system utilizes a high-pressure, non-metallic sand-packed tube made of polyether ether ketone (PEEK), with an inner diameter of 18 mm and a sand-packed section length of 60 mm. The designed operating pressure does not exceed 15 MPa (accuracy ±0.1%), and the working temperature does not exceed 90°C (accuracy ±0.01°C). In the experimental setup, temperature regulation is accomplished via a circulating bath capable of maintaining temperatures from −20°C to 40°C, with a precision of ±0.01°C. The temperature control medium is fluorinated oil (FC-40, 3M, USA), which contains no $^{1}H$ nuclei, thereby avoiding interference with NMR signal detection (Zhao YC et al., 2023). The pressure control unit utilizes a high-pressure syringe pump that enables real-time pressure monitoring and adjustment, injecting methane gas into the sand-packed tube to simulate the *in-situ* pressure conditions of hydrate reservoirs. By integrating temperature and pressure control with NMR imaging technology, this system enables real-time monitoring of drilling fluid invasion under simulated hydrate reservoir conditions and dynamic evaluation of the temporary plugging performance of thermoresponsive temporary plugging agents.

*2.5.2. Experimental procedure*

Based on the NMR analysis platform, the plugging and self-removal performance of the thermoresponsive temporary plugging agent was evaluated. The specific experimental procedure is as follows.

(i) Preparation of the hydrate-bearing sediment layer. Hydrate synthesis took place within a porous medium. Based on the particle size distribution typical of South China Sea marine sediments, quartz sand in the 80–100 mesh range was chosen as the packing material. According to the predetermined water content, 23 g of quartz sand and 3 g of ultrapure water were thoroughly mixed and packed into a high-pressure sand-packed NMR tube. The tube was then fixed in the experimental chamber of the NMR instrument, and all relevant pipelines were connected and checked for air tightness. Subsequently, a vacuum pump was used to evacuate the tube to remove residual air. The confining pressure pump was started, and fluorinated oil was injected into the coolant reservoir. The confining pressure was then set to 2 MPa. The outlet valve was opened, the backpressure was adjusted to 6 MPa, and high-purity methane gas was injected at a rate of 0.2 mL/min. After the pressure in the NMR tube stabilized at 6 MPa, the inlet valve was closed.

(ii) Hydrate formation stage. The temperature control circulation system was activated to lower the temperature of the sand-packed tube to 2.0°C. The temperature, pressure, and other parameters within the tube were monitored and recorded in real-time. Hydrate formation was considered complete when the pressure drop rate decreased to less than 0.02 MPa/h.

(iii) Fluid invasion into the hydrate-bearing sediment layer. After hydrate formation was stabilized, the backpressure valve was adjusted to reduce the pressure inside the tube to 4 MPa. Subsequently, 200 mL of ultrapure water and 200 mL of a 2% TRP solution were separately injected into an intermediate container. The temperature of the intermediate container was raised to 16°C, which is above the LCST of TRP. A plunger pump was used to inject the solutions sequentially into the hydrate-bearing sediment layer at a steady flow rate of 2 mL/min. Throughout this process, both temperature and the inlet/outlet pressures of the sand-packed tube were continuously monitored. Nuclear magnetic resonance scans were utilized to track dynamic variations in water content within the pore structure of the hydrate sediment. The invasion behavior of pure water and TRP solution was compared. The plugging effectiveness of the thermoresponsive temporary plugging agent on hydrate-bearing sediment was evaluated based on variations in the inlet/outlet pressure difference and water saturation of the sediment layer.

(iv) Cooling-induced plug removal. During the hydrate production stage, depressurization is commonly used as the primary recovery technique. The decomposition of hydrates is an endothermic process, resulting in a decrease in reservoir temperature (Qin XW et al., 2024). To simulate the plug removal process during hydrate production, cold water at 10°C was injected into the sand-packed tube in reverse at a flow rate of 1 mL/min. The NMR signals and the changes in inlet/outlet pressure within the tube were recorded simultaneously. By comparing the pore water distribution images and the pressure differences before and after plug removal, the performance of the thermoresponsive temporary plugging agent in plug removal was quantitatively analyzed.

*2.6. Mechanism analysis of TRP*

*2.6.1. Factors affecting the LCST*

Marine gas hydrate reservoirs are typically found in shallow and deepwater environments characterized by low temperatures and high salinity of pore fluids (Liao B et al., 2023b). The phase transition temperature of thermoresponsive polymers is affected by both the polymer and salt concentrations. To examine how varying polymer amounts impact the LCST of TRP, aqueous solutions containing TRP at mass fractions of 1%, 1.5%, 2%, 2.5%, and 3% were prepared at 10°C. The solutions were gradually heated, and their LCST values were measured using a UV-Visible spectrophotometer. Meanwhile, to study the effect of salt concentration on the LCST of TRP, a 2% TRP solution was prepared, and the NaCl concentrations in the solution were adjusted to 4%, 6%, 8%, 10%, and 12%, respectively. The LCST values were then determined using UV-Visible spectrophotometry.

*2.6.2. Scanning electron microscopy (SEM) analysis of filter cakes*

A model 450 scanning electron microscope (FEI Technology Co., Ltd., USA) was utilized to investigate the microstructure of filter cakes generated from bentonite

slurries, both with and without 2% TRP addition. A conductive metal layer was applied to the surface of each filter cake; the sample surface was subsequently examined and recorded by scanning it with an electron beam to reveal the filter cake's micro-morphology.

*2.6.3. Contact angle analysis of rock samples*

Deep-sea soil samples treated with either TRP solution or pure water were compressed into cylindrical rock specimens with smooth surfaces using a YPJ-40T tablet press. The water contact angle (WCA) on the surface of each rock sample was measured using an OCA25 optical contact angle measuring instrument (Dataphysics, Germany). At least five points from different regions of each sample were tested, and the average value was calculated to evaluate the surface properties of the rock samples under the two different treatment conditions.

## 3. Results and discussion

### *3.1. Structural characterization of TRP*

The structural characterization of TRP was conducted using Fourier transform infrared (FTIR) spectroscopy, UV-Visible spectroscopy, particle size distribution analysis, and zeta potential analysis. The specific results are presented in Fig. 3.

*3.1.1. Infrared spectral analysis*

TRP was synthesized via free radical polymerization for use in deep-sea, low-temperature natural gas hydrate drilling fluids. The synthetic route of the reaction product is shown in Fig. 1, and the FTIR spectrum of the prepared copolymer is presented in Fig. 3a. As shown in Fig. 3a, the absorption peaks at 1040 $cm^{-1}$ and 1190 $cm^{-1}$ are characteristic of the S=O bonds in the sulfonate group of the AMPS monomer. The peak at 627 $cm^{-1}$ corresponds to the stretching vibration of the S-O bond (Chang XF et al., 2019), while the peak at 1663 $cm^{-1}$ is attributed to the asymmetric stretching of the C=O bond in the amide group. The absorption at 3316 $cm^{-1}$ results from the N-H stretching vibration in the amide group, and the peak at 1545 $cm^{-1}$ arises from the coupling of the N-H bending vibration and C-N stretching vibration (Liu XD et al., 2004; Shahnazi A et al., 2020), which is another characteristic feature of the amide group. The peak at 1716 $cm^{-1}$ is due to the stretching vibration of the carbonyl (C=O) group in the ester moiety of BMA. The peaks at 2972 $cm^{-1}$ and 2930 $cm^{-1}$ are related to the stretching vibrations of C-H in the alkyl chains, mainly from methyl and methylene groups. The adjacent double peaks at 1367 $cm^{-1}$ and 1387 $cm^{-1}$ result from the coupling and splitting of the symmetric deformation vibration of the two methyl groups in the isopropyl group. The foregoing analysis demonstrates that amide and sulfonic acid functional groups have been effectively introduced into the thermoresponsive polymer, confirming that the obtained material aligns with the intended molecular design specifications.

*3.1.2. UV-Visible spectroscopy analysis*

The thermoresponsive properties of TRP were evaluated using a UV-Visible spectrophotometer, and the results are shown in Fig. 3b. At temperatures lower than the LCST, the polymer is fully dissolved in water, and the solution remained clear and transparent. As the temperature gradually increased

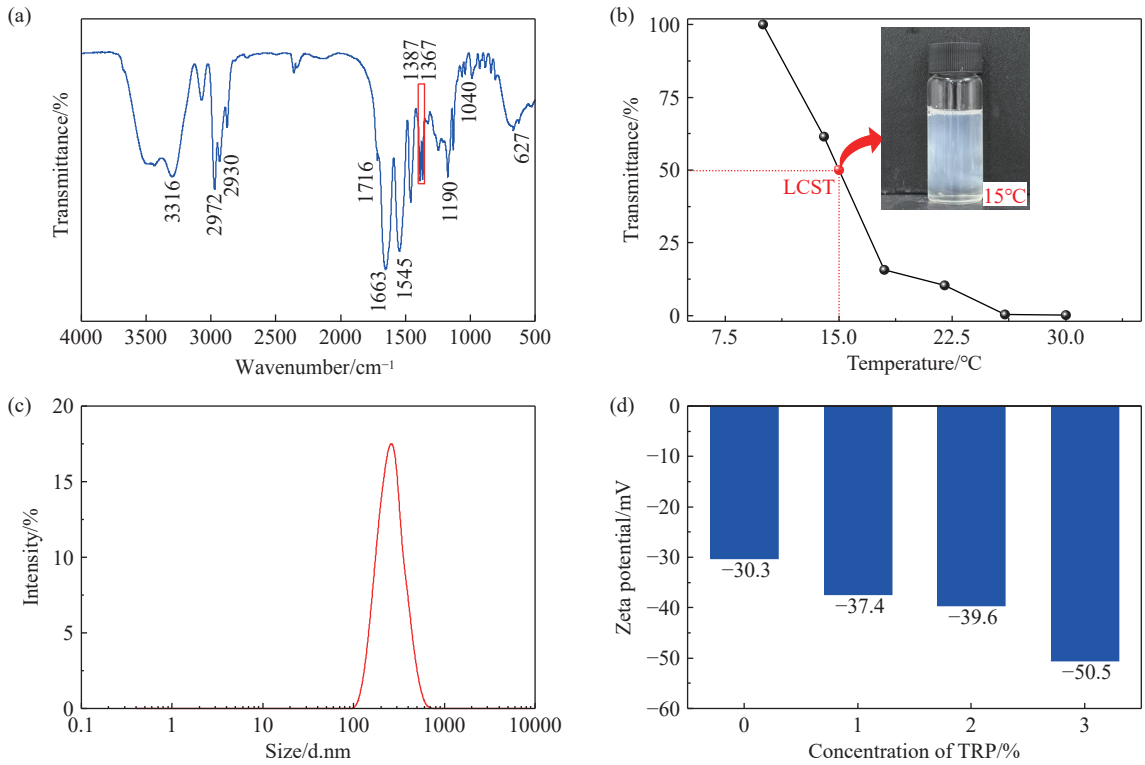


**Fig. 3.** Structural characterization of TRP. a–Fourier transform infrared (FTIR) spectroscopy analysis; b–characterization of the thermoresponsive point; c–particle size distribution; d–zeta potential analysis.

to the LCST, the polymer underwent phase separation and precipitation, resulting in a decrease in solution transparency. As the temperature continued to rise, the color of the solution shifted from light blue to a milky white, illustrating pronounced thermoresponsive characteristics. Instrumental analysis indicates that, at a TRP concentration of 2%, the temperature at which the transmittance decreases to 50% of its initial value is 15°C. According to the LCST definition described in Section 2.3.2, this confirms that the LCST of TRP is approximately 15°C under the tested concentration. By comparing the performance of the TRP with other reported thermoresponsive polymers (Table 2), this study notes that the TRP synthesized has an LCST of about 15°C, which is better aligned with the temperature conditions of hydrate reservoirs in the South China Sea and allows for a broader range of operating scenarios (Wei JG et al., 2019; Ye JL et al., 2019; Qin XW et al., 2020).

*3.1.3. Particle size distribution and zeta potential analysis*

The plugging characteristics of nanoparticles in formations are often closely related to their particle size distribution (Qiu ZS et al., 2018). A 0.05 mg/mL TRP aqueous solution was analyzed with a nanoparticle size and zeta potential analyzer to evaluate its properties above the LCST. The results are shown in Fig. 3c. The particle size distribution curve indicates that when the temperature is above the LCST, TRP precipitates in the form of nanoparticles in aqueous solution, with an average particle size ($D_{ave}$) of 266.89 nm and a polydispersity index (PDI) of 0.06, suggesting a uniform particle size distribution. Zeta potential is a key parameter that reflects the surface charge state of particles and directly influences the stability of drilling fluids. Elevated absolute zeta potential values correspond to increased electrostatic repulsion among particles, resulting in better dispersion in the drilling fluid. Using a specialized sample cell, the zeta potential values of 4% bentonite slurry containing different concentrations of TRP were measured, as shown in Fig. 3d. With increasing TRP concentration, the absolute value of the zeta potential of the bentonite slurry system gradually increased, reaching a maximum absolute value of 50.5 mV at a TRP concentration of 3%, indicating optimal dispersion and stability of the system at this concentration.

**Table 2. Comparison of LCST among different thermoresponsive polymers.**

| Thermoresponsive polymers | LCST/°C | References |
|---|---|---|
| poly(N-vinylcaprolactam-co-vinyl acetate) (PNVCL+VAC) | 19 | Halligan E et al., 2023 |
| poly(2-ethoxyethyl vinyl ether) (PEOVE) | 20 | Aoshima S et al., 1992 |
| poly(N-isopropylacrylamide) (PNIPAM) | 32 | Li X et al., 2023 |
| HTSP | 18 | Li X et al., 2023 |
| This study | 15 | |

*3.2. Performance evaluation of TRP*

When drilling operations are conducted in marine gas hydrate reservoirs, the plugging performance of drilling fluids is crucial for effectively sealing microfractures and pores in the reservoir, inhibiting fluid invasion-induced hydrate phase instability and wellbore collapse (Wang JT et al., 2023; Zhao K et al., 2025). It is a key technical factor for maintaining reservoir integrity and reducing well control risks. Increasing the dosage of the thermoresponsive temporary plugging agent TRP has little effect on the rheological properties of the slurry, indicating good compatibility between TRP and the bentonite slurry system. The plugging performance evaluation results are presented in Fig. 4.

As shown in Fig. 4a, TRP can deposit within the filter membrane pores to form a dense filter cake, significantly reducing pore permeability. When the TRP dosage was 1%, the fluid loss at 25°C decreased by 38.2%. Under low-temperature conditions of 4°C, it further decreased to 42.6%, demonstrating excellent plugging performance and adaptability to low temperatures. Fig. 4b shows that the addition of 2% TRP, 2% ultrafine $CaCO_3$, and 2% nano-emulsion all markedly suppressed the fluid loss of the bentonite slurry, significantly improving the plugging performance of the system. Among them, the addition of TRP produced the most significant plugging effect, with a cumulative 30-minute fluid loss reduction of 27.7% compared to the bentonite slurry. This superior plugging ability is

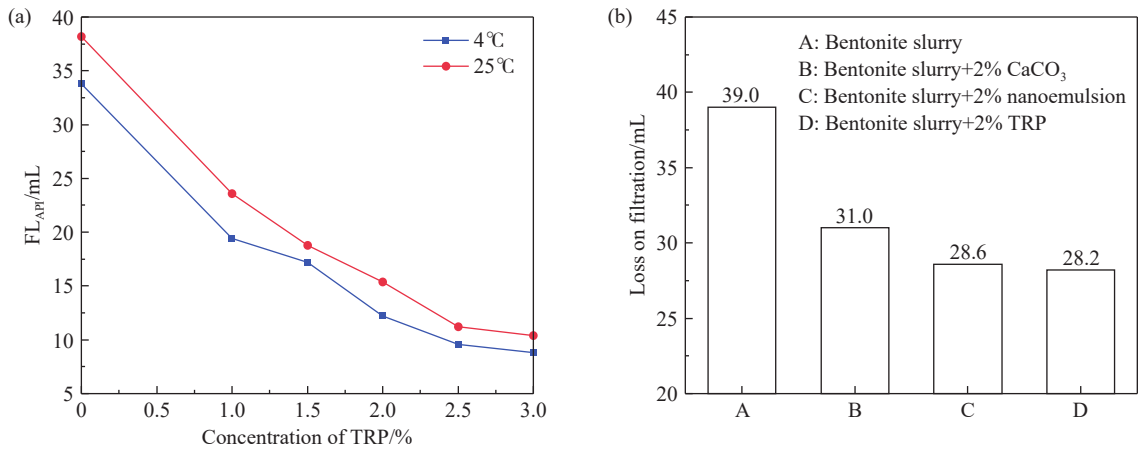


**Fig. 4.** Performance evaluation of TRP. a–Filtration performance evaluation; b–sand-disk plugging performance.

attributed to the rapid self-assembly of TRP molecular chains into nanoscale aggregates on the surface of pores or filter membranes above the LCST. This process is driven by the breaking of hydrogen bonds in the -CONH- groups and subsequent hydrophobic association, resulting in the formation of a dense filter cake and highly efficient plugging of channels.

### *3.3. Evaluation of the temporary plugging performance of TRP in simulated hydrate-bearing formations*

Utilizing the low-field nuclear magnetic resonance (NMR) imaging platform (see Fig. 2), the full sequence of drilling fluid intrusion into hydrate-rich reservoirs was modeled to comprehensively assess the temporary sealing effectiveness of the thermoresponsive plugging agent TRP. This provides experimental evidence for wellbore stability and reservoir protection in gas hydrate-bearing formations.

#### *3.3.1. Hydrate formation simulation*

Natural gas hydrate formation was simulated using a sand-packed tube, beginning at an initial pressure of 6 MPa and a temperature of 20°C. Fig. 5 illustrates the real-time variations in both temperature and pressure inside the tube. After about 2 hours of cooling, the temperature dropped from 20.5°C to 2.0°C, while the pressure decreased from 6.1 MPa to 5.5 MPa, signaling the onset of rapid hydrate generation. Following approximately 9 hours of continuous reaction, both temperature and pressure gradually stabilized, with the pressure drop rate falling below 0.02 MPa/h, ultimately maintaining values of approximately 1.9°C and 4.98 MPa. This indicates that the hydrate formation process was essentially complete (Wang JT et al., 2024c).

During the hydrate formation process, magnetic resonance imaging (MRI) images of the sediment layer at different time points (Fig. 6) and the evolution curves of the $T_2$ spectra (Fig. 7) were simultaneously recorded, allowing for the observation of changes in the pore structure and the state of water occurrence. Based on the changes in NMR signal intensity, combined with the trends in temperature and pressure within the sand-packed tube and using the conversion formulas relating NMR imaging intensity to water saturation and

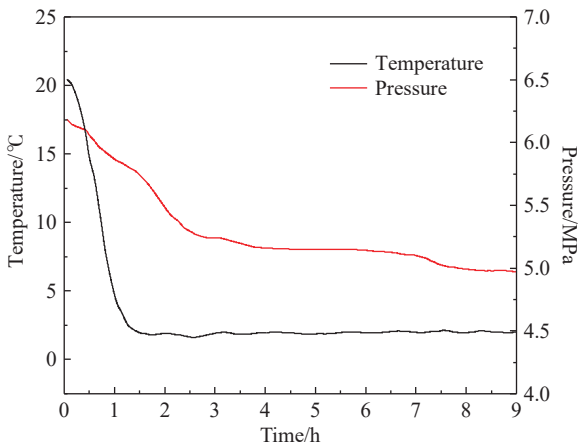


**Fig. 5.** Temperature-pressure profiles during hydrate generation.

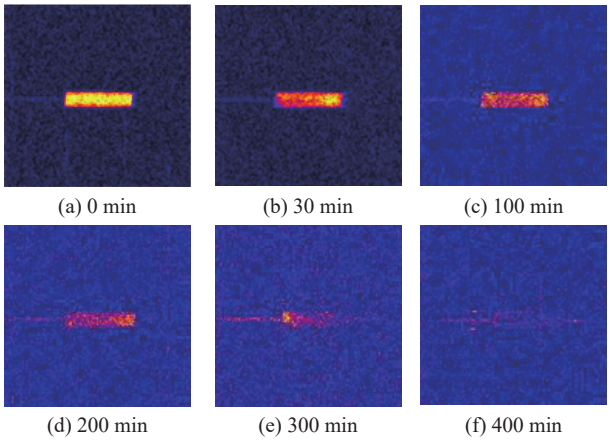


**Fig. 6.** Nuclear magnetic resonance imaging results during hydrate generation.

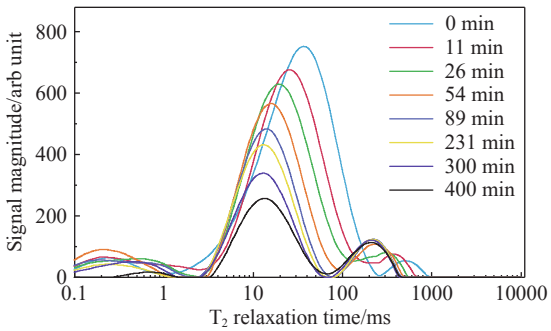


**Fig. 7.** $T_2$ spectra during hydrate generation.

hydrate saturation in the sediment (Shao ZH et al., 2023), it was determined that the initial water saturation of the sediment was 50.3%. After hydrate formation stabilized, the hydrate saturation of the sediment reached 56.4%, while the residual water saturation decreased to 5.27%. This indicates that a substantial amount of pore water in the sediment participated in the hydrate formation reaction under sufficient methane gas conditions. The free pore water was gradually consumed, leading to significant changes in the pore structure and fluid occurrence state of the sediment, and the hydrate was uniformly distributed within the artificial core.

The $T_2$ spectrum reflects the transverse relaxation characteristics of pore water in porous media, with the area under the curve representing the pore water content. In the initial stage, free water was uniformly distributed within the sediment, as indicated by a dominant free water peak in the $T_2$ spectrum corresponding to a relatively long relaxation time (approximately 117 ms), suggesting that pore water was mainly present as free water at this stage (Liu Z et al., 2023). As the reaction progressed, the $T_2$ spectrum shifted toward the short-relaxation region, and the 117 ms free water peak rapidly decayed, indicating that free water continuously participated in hydrate formation and was gradually replaced by hydrate crystals. The observed trends —attenuation of image brightness, reduction in $T_2$ area, and transformation of pore water —were highly consistent, reflecting a close coupling among the changes in pore water occurrence, pore structure evolution, and hydrate formation throughout the

hydrate generation process.

*3.3.2. Evaluation of plugging performance during drilling fluid invasion*

To evaluate the plugging performance of TRP under simulated hydrate reservoir conditions, the invasion processes of pure water and TRP solution into the hydrate-bearing sediment layer were monitored using a low-field NMR imaging system (Fig. 8). The results showed that pure water rapidly invaded the sediment along high-permeability channels, continuously inducing hydrate dissociation and releasing large amounts of free water, as evidenced by a significant increase in MRI signal intensity. This process compromised the structural stability of the reservoir. In contrast, the TRP solution was able to quickly form a dense and stable plugging layer near the injection inlet during invasion, effectively restricting further fluid penetration. The invasion front of the TRP solution ultimately stabilized at approximately 15 mm from the outlet of the sand-packed tube, and the MRI signal intensity remained essentially unchanged over a prolonged period (>200 min), demonstrating excellent plugging persistence and stability. This temporary plugging effect can be maintained over the long term, effectively reducing the risk of hydrate dissociation caused by the invasion of drilling fluid.

The variations in the inlet/outlet pressure differential and water saturation within the sediment layer during the invasion processes of pure water and TRP solution are shown in Fig. 9. When pure water was injected, the pressure differential across the sand-packed tube remained at approximately 0.1 MPa, and the water saturation in the sediment layer rapidly increased to 83%, indicating that pure water could easily penetrate deep into the sediment and exhibit a broad fluid penetration range. In contrast, the TRP solution rapidly formed a high-strength plugging barrier at the initial stage of injection, causing the inlet/outlet pressure differential to rise quickly to 6 MPa within 12 minutes and effectively preventing further fluid invasion. After 10 minutes of injection, the water saturation in the sediment layer stabilized at approximately 32.5%, and even with continuous injection at a constant pressure of 6 MPa, it increased by only 2.1%. This stable plugging process demonstrates that TRP exhibits excellent compatibility with the pore structure of the sediment, and the formed plugging layer possesses outstanding sustained plugging capacity and pressure-bearing performance under high differential pressure conditions. As a result, the invasion depth of the drilling fluid

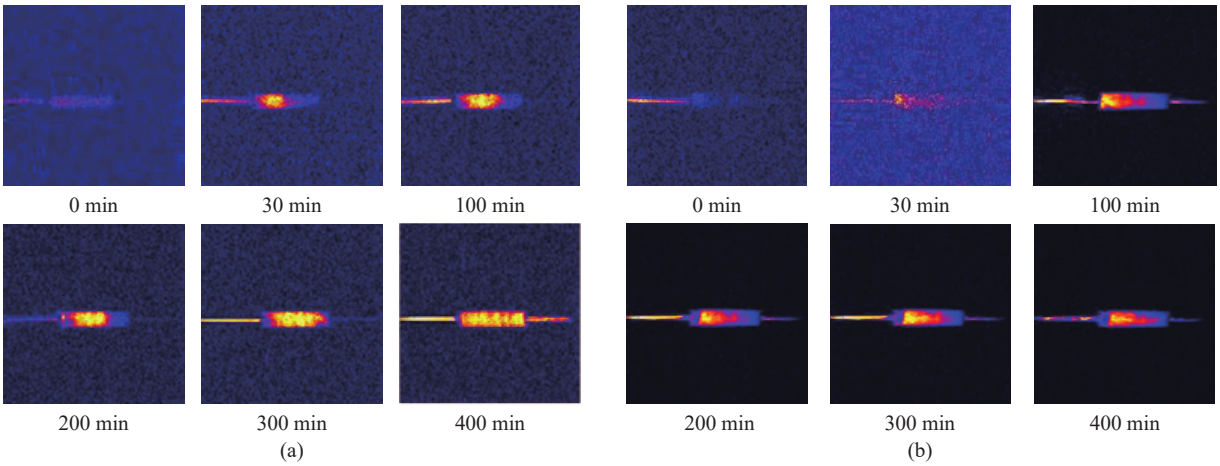


**Fig. 8.** NMR imaging results of fluid invasion into the hydrate-bearing reservoir. a–Pure water; b–TRP solution.

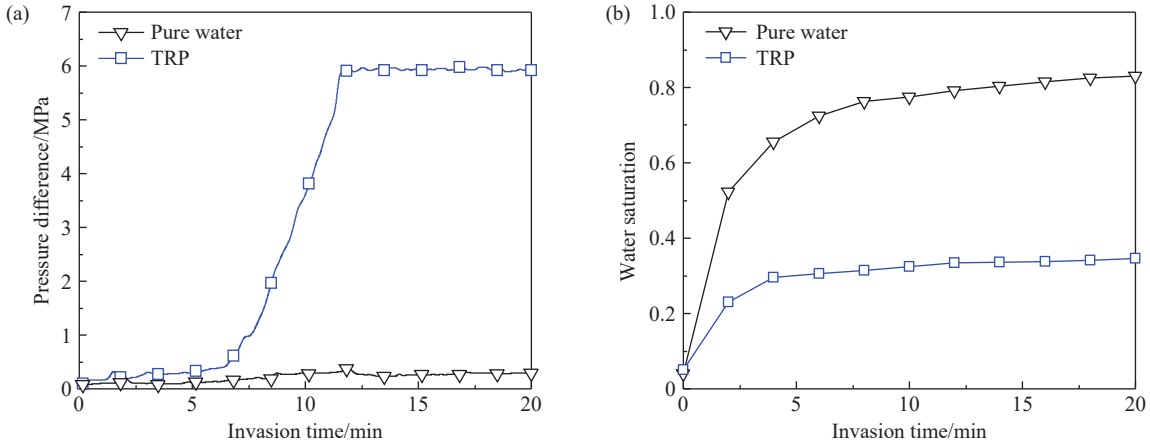


**Fig. 9.** Parameter changes during fluid invasion into the hydrate-bearing reservoir. a–Variation of inlet/outlet pressure differential in the sand-packed tube; b–change in water saturation of hydrate-bearing sediments.

and the risk of hydrate dissociation are significantly reduced, enabling effective protection of the hydrate reservoir.

*3.3.3. Evaluation of plug removal performance of drilling fluids*

During drilling, TRP can plug the formation and thus maintain wellbore stability; however, it may also reduce reservoir permeability, consequently decreasing gas production during hydrate development. Therefore, it is also necessary to evaluate its reversible plug removal performance. The plug removal performance of TRP was evaluated by simulating the reservoir cooling process during depressurization-based hydrate production using reverse injection of cold water at 10°C. The MRI images of the sediment layer and the variation in the inlet/outlet pressure differential of the sand-packed tube during the reverse injection process are shown in Fig. 10 and Fig. 11, respectively. The experimental results indicate that, during the initial stage of reverse injection (the first 18 minutes), the pressure differential across the sand-packed tube remained at approximately 3.8 MPa, demonstrating that the temporary plugging layer formed by TRP still maintained high plugging strength, preventing further invasion of cold water into the reservoir. As cold water injection continued and the reservoir temperature gradually dropped below the LCST of TRP, the thermoresponsive polymer particles in the temporary plugging layer gradually dissolved. The dissolved polymer was carried away, and the pore channels were progressively reopened, resulting in a gradual recovery of sediment permeability. After 18 minutes, the inlet/outlet pressure differential rapidly decreased and stabilized at approximately 0.12 MPa, indicating that the temporary plugging layer had been essentially removed. According to calculations based on Darcy's law, the reservoir permeability at this stage was restored to as high as 96.8%. The bright region in the MRI images also gradually extended deeper into the reservoir and eventually became uniformly distributed, further confirming that TRP exhibits excellent self-removal capability and reversible thermoresponsive behavior under low-temperature conditions. These findings highlight the significant application potential of TRP for drilling and reservoir protection in marine gas hydrate reservoirs.

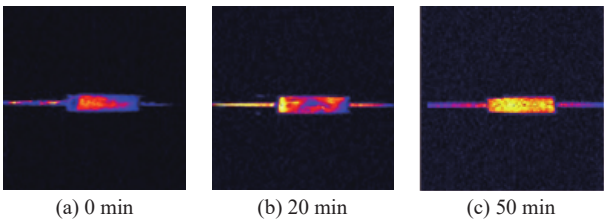


**Fig. 10.** MRI imaging results of hydrate reservoirs during reverse injection of cold water.

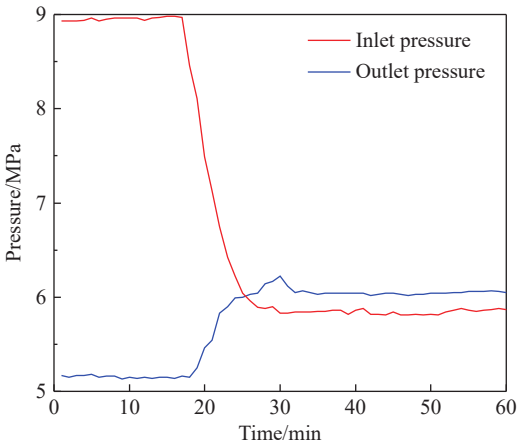


**Fig. 11.** Pressure changes in the inlet and outlet of the sand-packed tube during reverse injection of cold water.

*3.4. Mechanism analysis of TRP*

*3.4.1. Factors affecting the LCST*

Both the polymer content and the salt level generally affect the phase transition temperature of thermoresponsive polymers (Costa MC et al., 2015; Liao B et al., 2023a). Fig. 12 presents the influence of polymer dosage and salt concentration on the LCST of TRP. Experimental results indicate that as the polymer concentration increases from 1% to 3%, the LCST of TRP decreases only slightly, from 15.8°C to 14.7°C, suggesting that polymer concentration has a minimal effect on the phase transition temperature. This slight decrease is mainly attributed to the enhanced hydrophobic interactions within the polymer chains at higher

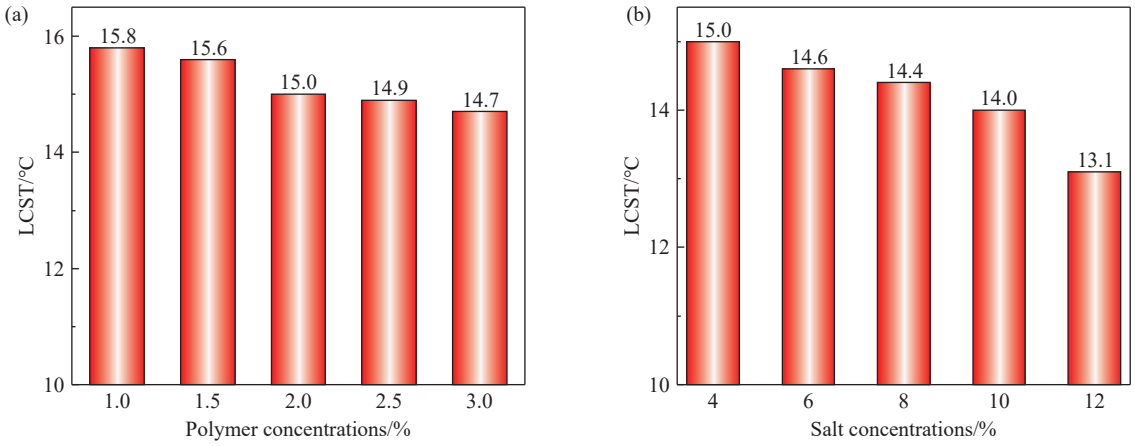


**Fig. 12.** Effect of concentration on the LCST of TRP. a–Polymer concentration; b–salt concentration.

concentrations, where intermolecular association inhibits hydrogen bonding with water, thereby marginally lowering the phase separation temperature. In contrast, salt concentration has a significantly more pronounced effect on the LCST: As the salt concentration rises from 4% to 12%, the LCST drops from 15.0°C to 13.1°C. This phenomenon occurs because salt ions interfere with the hydration interactions between polymer chains and water molecules, diminishing both the hydration capacity and the electrostatic repulsion among polymer chains, which in turn facilitates hydrophobic aggregation of the chain segments. As a result, the phase transition occurs more readily at lower temperatures, further decreasing the LCST value. This salt-induced decrease in LCST is particularly relevant to hydrate-bearing sediments, where pore fluids may exhibit elevated salinity due to ion enrichment during hydrate formation. Therefore, the effective phase-transition temperature of TRP under field conditions may be slightly lower than that measured in pure-water systems, and salinity effects should be considered when designing TRP formulations for hydrate drilling fluids.

*3.4.2. Scanning electron microscopy (SEM) analysis of filter cakes*

SEM was used to analyze the microstructure of filter cakes prepared from bentonite slurries with and without the addition of 2% TRP at a magnification of 3000×, as shown in Fig. 13. The SEM images reveal that the surface of the filter cake without TRP is relatively rough and contains noticeable pores. In contrast, the filter cake with 2% TRP exhibits a much smoother, denser surface with significantly fewer pores, indicating that TRP can fill and seal the micro-pores within the filter cake, thereby markedly improving its compactness. This modification significantly lowers the filter cake's permeability, indicating that TRP is crucial for effective plugging and for improving the structural stability of the filter cake.

*3.4.3. Water contact angle (WCA) analysis of rock samples*

WCA analysis was performed on rock samples treated with TRP to directly quantify the change in surface wettability before and after the phase transition, thereby verifying the thermoresponsive mechanism of plugging via hydrophobization and unplugging via rehydration. The specific experimental results are shown in Fig. 14. The results indicate that, after treatment with 2% TRP, the water contact angle on the rock surface increased from 41.5° to 77.4°. This suggests that, above the LCST of TRP, the hydrogen bonds between the -CONH- carbonyl groups and water molecules are broken, and the polymer chains curl up and self-assemble through hydrophobic side-chain association to form a dense nanofilm. The exposed isopropyl groups and hydrophobic network are reconstructed on the rock substrate, significantly enhancing surface hydrophobicity and effectively preventing the spreading and adsorption of water within pores and fractures.

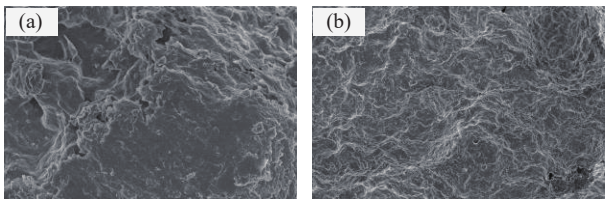


**Fig. 13.** SEM images of filter cakes at 3000× magnification. a–Filter cake without TRP; b–filter cake with 2% TRP.

Based on the SEM analysis of filter cakes and the contact angle measurements of rock samples, the mechanisms of plugging and unplugging by the thermoresponsive temporary plugging agent during drilling in natural gas hydrate reservoirs are illustrated in Fig. 15.

As illustrated in Fig. 15, the thermoresponsive temporary plugging agent can undergo phase transitions in response to temperature changes within the wellbore during marine gas hydrate drilling, thereby achieving both plugging and unplugging of the hydrate reservoir. During the drilling process, if the wellbore temperature exceeds the phase transition temperature of the plugging agent, the thermoresponsive agent stays evenly dispersed in the drilling fluid as nanoparticles. Upon reaching the target reservoir, under a positive pressure differential, these nanoparticles migrate into microfractures and pores within the reservoir, gradually accumulating to form a dense plugging layer at the interface between the reservoir and the wellbore. This effectively prevents drilling fluid loss into the reservoir, reduces formation disturbance, and protects the integrity of the hydrate reservoir. During hydrate production, when the reservoir temperature drops below the LCST of the thermoresponsive plugging agent, the nanoparticles undergo a reversible phase transition and re-dissolve into the aqueous phase, thereby removing the plugging layer and restoring reservoir permeability.

From a molecular perspective, the reversible "plugging-unplugging'' behavior illustrated in Fig. 15 is primarily governed by the hydrophilic-hydrophobic balance of the polymer chains, which is driven by the competition between conservative repulsive forces and electrostatic attractions within the chain segments. This competition determines chain contraction or extension and consequently regulates the plugging state of the formation, consistent with the recent dissipative particle dynamics (DPD) simulations reported by Zhu B et al. (2024a, 2024b). When the temperature exceeds the LCST, hydrogen bonds between the -CONH- groups and surrounding water molecules break, leading to the collapse of

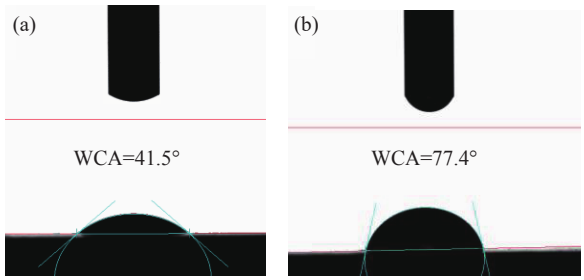


**Fig. 14.** WCA of the rock samples before and after TRP treatment. a–Contact angle of rock samples after pure water treatment; b–contact angle of rock samples after TRP treatment.

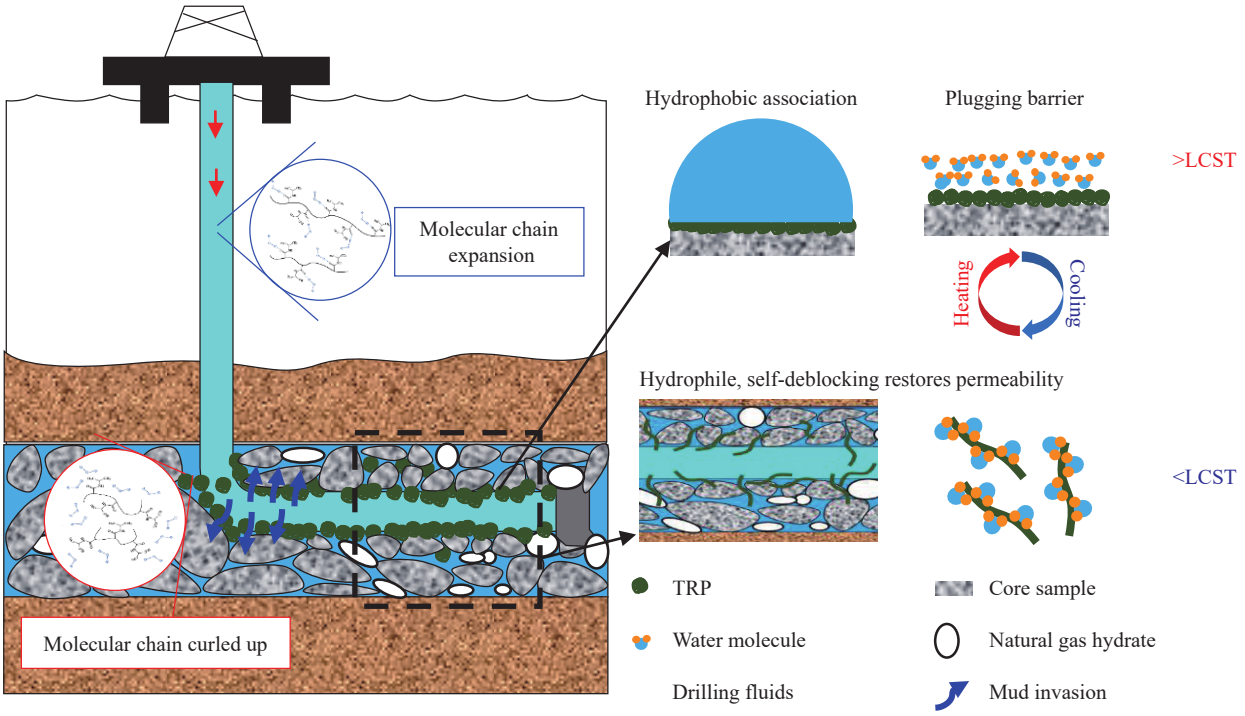


**Fig. 15.** Schematic diagram of the action mechanism of thermoresponsive temporary plugging agent (TRP).

the hydration layer. This triggers a coil-to-globule conformational transition of the NIPAM-based chains and promotes hydrophobic association among side groups, resulting in dense nanoparticle aggregates capable of effectively sealing pore spaces. Conversely, when the temperature falls below the LCST, hydration around the polymer chains is restored, hydrophobic clusters dissociate, and the temporary plugging layer redissolves. Therefore, the macroscopic plugging-unplugging behavior of TRP essentially originates from reversible conformational transitions and the switching of intermolecular interactions at the molecular scale, representing a temperature-induced adaptive phase-transition mechanism. Based on this mechanism, TRP can effectively plug the formation, prevent drilling-fluid invasion, and enhance wellbore stability during drilling, while during hydrate production it can self-remove as the temperature decreases, thereby improving production efficiency and enabling the safe and efficient development of deep-sea natural gas hydrates.

## 4. Conclusions

In this study, to address the challenges of wellbore instability and reservoir damage encountered during drilling in marine gas hydrate reservoirs, a polymer-based temporary plugging agent (TRP) with thermoresponsive properties was successfully designed and synthesized. Through systematic structural characterization, performance evaluation, and mechanistic analysis, the following conclusions were drawn.

(i) Structural characterization confirmed the successful incorporation of amide and sulfonic acid groups into TRP, consistent with the intended molecular design. TRP exhibited pronounced thermal responsiveness (LCST ≈ 15°C), which matches the temperature of gas hydrate reservoirs in the South China Sea. When the temperature exceeded the LCST, TRP underwent thermally induced aggregation to form nanoparticles with an average particle size of approximately 267 nm and a uniform size distribution (PDI = 0.06). The addition of 3% TRP increased the absolute value of the zeta potential in the bentonite-based drilling fluid to 50.5 mV, significantly improving the dispersion stability and anti-agglomeration capability of the system.

(ii) Performance evaluation results demonstrated that TRP exhibited excellent low-temperature temporary plugging performance. At a dosage of 1%, the API fluid loss was reduced by 38.2% at 25°C and by 42.6% at 4°C. With a 2% dosage, sand-disk simulation tests showed that the cumulative 30-min fluid loss decreased by 27.7% compared with the base slurry, outperforming ultrafine calcium carbonate and nano-emulsion. Low-field NMR measurements further demonstrated that TRP rapidly formed a high-strength temporary plugging layer in the sand-packed column during fluid invasion, causing the inlet/outlet differential pressure to rise to 6 MPa within 12 min and remain stable for 200 min. Upon cooling below the LCST, the permeability of the sediment recovered to 96.8%, confirming the excellent reversible self-removal capability of TRP.

(iii) Mechanistic analysis revealed that the thermoresponsive plugging performance of TRP derives from the synergistic effect of the amide and sulfonic acid groups in its molecular structure. Above the LCST, hydrophobic associations among polymer chains form a dense network structure, constructing a hydrophobic film on pore surfaces, which enhances filter cake compactness and core surface hydrophobicity, effectively preventing drilling fluid invasion and damage to the hydrate reservoir. Upon cooling, TRP nanoparticles rapidly disassemble and re-dissolve, reopening the formation permeability pathways and achieving dynamic

reservoir protection.

In summary, the TRP developed in this study exhibits outstanding thermoresponsive reversibility and plugging performance, effectively reducing wellbore instability and reservoir damage risks during drilling in hydrate-bearing formations. These findings provide new insights and practical guidance for the design and application of intelligent adaptive temporary plugging agents. Despite its promising potential, several limitations remain —most notably the lack of a quantitative molecular-level model for nanoparticle aggregation dynamics and the need to validate TRP performance under more complex, field-relevant hydrate reservoir conditions. Future work should integrate molecular simulations with multi-scale experiments to further optimize the LCST characteristics of TRP, and conduct field-scale evaluations under real downhole conditions to promote the practical deployment of thermoresponsive agents for safe and efficient deep-sea gas hydrate drilling and production.

## CRediT authorship contribution statement

Jin-tang Wang and Ke Zhao conceived of the presented idea. All authors discussed the results and contributed to the final manuscript.

## Declaration of competing interests

The authors declare no conflicts of interest.

## Acknowledgment

The author thanks the reviewers who participated in the manuscript review. This study was supported by the National Natural Science Foundation of China (52274025), the Key R&D Program of Shandong Province, China (2024CXPT076) and the Taishan Scholar Plan Project in Shandong Province (tsqn202408090).

## References

Aoshima S, Oda H, Kobayashi E. 1992. Synthesis of thermally-induced phase separating polymer with well-defined polymer structure by living cationic polymerization. I. Synthesis of poly(vinyl ether)s with oxyethylene units in the pendant and its phase separation behavior in aqueous solution. Journal of Polymer Science Part A: Polymer Chemistry, 30(11), 2407–2413. doi: 10.1002/pola.1992.080301115.

Chang XF, Sun JS, Xu Z, Lü KH, Dai ZW, Zhang F, Huang XB, Liu JP. 2019. Synthesis of a novel environment-friendly filtration reducer and its application in water-based drilling fluids. Colloids and Surfaces A: Physicochemical and Engineering Aspects, 568, 284–293. doi: 10.1016/j.colsurfa.2019.01.055.

Costa MCM, Silva SMC, Antunes FE. 2015. Adjusting the low critical solution temperature of poly(N-isopropyl acrylamide) solutions by salts, ionic surfactants and solvents: A rheological study. Journal of Molecular Liquids, 210, 113–118. doi: 10.1016/j.molliq.2015.02.008.

Dong XQ, Jin BY, Liu YH, Qian XL, Yu FC. 2024. Experimental study on degradable PGA as temporary plugging agent in drilling fluids. Drilling Fluid & Completion Fluid, 41(2), 166–171 (in Chinese with English abstract). doi: 10.12358/j.issn.1001-5620.2024.02.004.

Ge XM, Liu JY, Fan YR, Xing DH, Deng SG, Cai JC. 2018. Laboratory investigation into the formation and dissociation process of gas hydrate by low-field NMR technique. Journal of Geophysical Research: Solid Earth, 123(5), 3339–3346. doi: 10.1029/2017JB014705.

Halligan E, Zhuo S, Colbert DM, Alsaadi M, Tie BSH, Bezerra GSN, Keane G, Geever LM. 2023. Modulation of the lower critical solution temperature of thermoresponsive poly(N-vinylcaprolactam) utilizing hydrophilic and hydrophobic monomers. Polymers, 15(7), 1595. doi: 10.3390/polym15071595.

Hsu SH, Yu TL. 2000. Dynamic viscoelasticity study of the phase transition of poly(N-isopropylacrylamide). Macromolecular Rapid Communications, 21(8), 476–480. doi: 10.1002/(SICI)1521-3927(20000501)21:8<476::AID-MARC476>3.0.CO;2-O.

Huang TJ, Zhang Y, Li G, Li XS, Chen ZY. 2020. Numerical modeling for drilling fluid invasion into hydrate-bearing sediments and effects of permeability. Journal of Natural Gas Science and Engineering, 77, 103239. doi: 10.1016/j.jngse.2020.103239.

Kubo M, Higuchi M, Koshimura T, Shoji E, Tsukada T. 2021. Control of the temperature responsiveness of poly (*N*-isopropylacrylamide-*co*-2-hydroxyethyl methacrylate) copolymer using ultrasonic irradiation. Ultrasonics Sonochemistry, 79, 105752. doi: 10.1016/j.ultsonch.2021.105752.

Li X, Huang WA, Zhen Z, Sun JS, Wang ZY, Maeda N. 2023. Preparation of thermo-responsive polymer and its application for plugging in hydrate-bearing sediments. Colloids and Surfaces A: Physicochemical and Engineering Aspects, 676, 132210. doi: 10.1016/j.colsurfa.2023.132210.

Liao YQ, Wang ZY, Chao MZ, Sun XH, Wang JT, Zhou BY, Sun BJ. 2021. Coupled wellbore–reservoir heat and mass transfer model for horizontal drilling through hydrate reservoir and application in wellbore stability analysis. Journal of Natural Gas Science and Engineering, 95, 104216. doi: 10.1016/j.jngse.2021.104216.

Liao B, Wang JT, Han XP, Wang R, Lv KH, Bai YJ, Jiang HY, Shao ZH, Wang YD, Sun JS. 2022. Microscopic molecular insights into clathrate methane hydrates dissociation in a flowing system. Chemical Engineering Journal, 430, 133098. doi: 10.1016/j.cej.2021.133098.

Liao B, Sun JS, Wang JT, Lü XD, Wang JL, Guo JX, Lv KH, Wang R, Zheng JJ, Chen ZX. 2023a. Development of novel natural gas hydrate inhibitor and the synergistic inhibition mechanism with NaCl: Experiments and molecular dynamics simulation. Fuel, 353, 129162. doi: 10.1016/j.fuel.2023.129162.

Liao B, Wang JT, Li MC, Lü KH, Wang Q, Li J, Huang XB, Wang R, Lv XD, Chen ZX, Sun JS. 2023b. Microscopic molecular and experimental insights into multi-stage inhibition mechanisms of alkylated hydrate inhibitor. Energy, 279, 128045. doi: 10.1016/j.energy.2023.128045.

Liu C, Wu XL, Ke X, Zeng XP, Wang DW, Wu JY. 2021. Progress in LCST smart polymers and their applications in biomedical field. Journal of Wuhan Institute of Technology, 43(1), 50–58 (in Chinese with English abstract). doi: 10.19843/j.cnki.cn42-1779/tq.202007004.

Liu XD, Xue WM, Liu Q, Yu WT, Fu YL, Xiong X, Ma XJ, Yuan Q. 2004. Swelling behaviour of alginate–chitosan microcapsules prepared by external gelation or internal gelation technology. Carbohydrate Polymers, 56(4), 459–464. doi: 10.1016/j.carbpol.2004.03.011.

Liu Z, Chen LT, Wang ZY, Gao YH, Wang JT, Yu CH, Sun BJ. 2023. Hydrate phase equilibria in natural sediments: Inhibition mechanism and NMR-based prediction method. Chemical Engineering Journal, 452, 139447. doi: 10.1016/j.cej.2022.139447.

Lou SF, Zhang H, Williams GR, Branford-White C, Nie HL, Quan J, Zhu LM. 2013. Fabrication and aggregation of thermoresponsive glucose-functionalized double hydrophilic copolymers. Colloids and Surfaces B: Biointerfaces, 105, 180–186. doi: 10.1016/j.colsurfb.2012.12.012.

Mu LF, Liu HT, Zhang C, Zhang Y, Lu HL. 2025. Optimization of production well patterns for natural gas hydrate reservoir: Referring to the results from production tests and numerical simulations. China Geology, 8(1), 39–57. doi: 10.31035/cg20230124.

Niu C, Fan S, Chen XP, He Z, Dai LY, Wen ZB, Li MC. 2024. Preparation and performance evaluation of a supramolecular polymer gel-based temporary plugging agent for heavy oil reservoir. Gels, 10(8), 536. doi: 10.3390/gels10080536.

Qin XW, Liang QY, Ye JL, Yang L, Qiu HJ, Xie WW, Liang JQ, Lu JA,

Lu C, Lu HL, Ma BJ, Kuang ZG, Wei JG, Lu HF, Kou BB. 2020. The response of temperature and pressure of hydrate reservoirs in the first gas hydrate production test in South China Sea. Applied Energy, 278, 115649. doi: 10.1016/j.apenergy.2020.115649.

Qin XW, Lu C, Wang PK, Liang QY. 2022. Hydrate phase transition and seepage mechanism during natural gas hydrates production tests in the South China Sea: A review and prospect. China Geology, 5(2), 201–217. doi: 10.31035/cg2022029.

Qin XW, Lu C, Zhang ZB, Wang PK, Li SD, Dong YH, Ma C, He YF, Pang SJ. 2024. Research progress on thermal-fluid coupling and temperature field regulation in natural gas hydrate production tests in the South China Sea. Acta Geologica Sinica, 98(11), 3213–3224 (in Chinese with English abstract). doi: 10.19762/j.cnki.dizhixuebao.2024514.

Qiu ZS, Xu JG, Yang P, Zhao X, Mou TB, Zhong HY, Huang WA. 2018. Effect of amphiphilic polymer/nano-silica composite on shale stability for water-based muds. Applied Sciences, 8(10), 1839. doi: 10.3390/app8101839.

Shahnazi A, Nabid MR, Sedghi R, Heidari B. 2020. A thermosensitive molecularly imprinted poly-NIPAM coated MWCNTs/$TiO_2$ photocatalyst for the preferential removal of pendimethalin pesticide from wastewater. Journal of Photochemistry and Photobiology A: Chemistry, 402, 112802. doi: 10.1016/j.jphotochem.2020.112802.

Shao ZH, Wang JT, Lv KH, Wang ZL, Bai YJ, Wang R, Sun JS. 2023. NMR based experiment of fluid invasion to natural gas hydrate reservoir and hydrate dissociation inhibition mechanism. Fuel, 354, 129372. doi: 10.1016/j.fuel.2023.129372.

Su PB, Wei W, Sun YB, Lü YY, Cheng H, Han WF, Zhang W, Liang JQ. 2024. Geological reservoir and resource potential ($10^{13}$ $m^3$) of gas hydrates in the South China Sea. China Geology, 7(3), 422–444. doi: 10.31035/cg2024069.

Suleimenov IE, Guven O, Mun GA, Uzun C, Gabrielyan OA, Kabdushev SB, Agibaeva L, Nurtazin A. 2017. Hysteresis effects during the phase transition in solutions of temperature sensitive polymers. Eurasian Chemico-Technological Journal, 19(1), 41–46. doi: 10.18321/ectj501.

Sun JS, Cheng YF, Qin XW, Sun YH, Jin Y, Wang ZY, Li SX, Lu C, Qu YZ, Lyu KH, Wang CW, Wang JT, Wang R. 2021. Research progress on natural gas hydrate drilling & production in the South China Sea. Bulletin of National Natural Science Foundation of China, 35(6), 940–951 (in Chinese with English abstract). doi: 10.16262/j.cnki.1000-8217.2021.06.014.

Sun JS, Li YY, Liao B, Bai YJ, Li WB, Xu JQ, Wang JT. 2024. Development and performance evaluation of bioenzyme-responsive temporary plugging materials. Advances in Geo-Energy Research, 11(1), 20–28. doi: 10.46690/ager.2024.01.03.

Wang JT, He ZJ, Sun J, Liu L, Li WB, Liao B, Zhao K, Li YY, Xu JQ. 2024a. Dynamics of horizontal well drilling in deepwater shallow gas hydrate reservoirs: A mass and heat transfer study. SPE Journal, 29(11), 6034–6049. doi: 10.2118/223589-pa.

Wang JT, He ZJ, Yan YC, Liu L, Yan J, Liao B, Zhao K, Li YY, Chen LQ. 2024b. Development of a dual-functional inhibitor for natural gas hydrates and construction of drilling fluid system. Gas Science and Engineering, 122, 205218. doi: 10.1016/j.jgsce.2024.205218.

Wang JT, Liao B, Liu L, Chen LQ, Huang YW, Zhao K, Sun XH, Lv KH, Zheng YX, Sun JS. 2024c. The effect of multi-component Inhibitor systems on hydrate formation. Gas Science and Engineering, 122, 205214. doi: 10.1016/j.jgsce.2024.205214.

Wang JT, Xu JQ, Liao B, Zhao K, Liu L, Bai YJ, Li WB, Jiang HY, Lv KH, Sun JS. 2023. Preparation and properties evaluation of multifunctional drilling fluid additive for marine natural gas hydrate. Drilling Engineering, 50(6), 11–17 (in Chinese with English abstract). doi: 10.12143/j.ztgc.2023.06.002.

Wang LS, Chow PY, Phan TT, Lim IJ, Yang YY. 2006. Fabrication and characterization of nanostructured and thermosensitive polymer membranes for wound healing and cell grafting. Advanced Functional Materials, 16(9), 1171–1178. doi: 10.1002/adfm.200500408.

Wang R, Liu TL, Ning FL, Ou WJ, Zhang L, Wang Z, Peng L, Sun JX, Liu ZC, Li TS, Sun HC, Jiang GS. 2019. Effect of hydrophilic silica nanoparticles on hydrate formation: Insight from the experimental study. Journal of Energy Chemistry, 30, 90–100. doi: 10.1016/j.jechem.2018.02.021.

Wang R, Wang C, Long YF, Sun JS, Liu LM, Wang JL. 2023. Preparation and investigation of self-healing gel for mitigating circulation loss. Advances in Geo-Energy Research, 8(2), 112–125. doi: 10.46690/ager.2023.05.05.

Wang XC, Sun YH, Li B, Zhang GB, Guo W, Li SL, Jiang SH, Peng SY, Chen HK. 2023. Reservoir stimulation of marine natural gas hydrate-a review. Energy, 263, 126120. doi: 10.1016/j.energy.2022.126120.

Wei AC, Liu SJ, Jiang DL, Liu PK, Zeng CM, Qiu ZS, Liu ZK. 2023. Synthesis and evaluation of epoxy resin self-degradation plugging agent for fractured formation. Drilling Fluid & Completion Fluid, 40(2), 163–168 (in Chinese with English abstract). doi: 10.12358/j.issn.1001-5620.2023.02.003.

Wei JG, Liang JQ, Lu JG, Zhang W, He YL. 2019. Characteristics and dynamics of gas hydrate systems in the northwestern South China Sea-Results of the fifth gas hydrate drilling expedition. Marine and Petroleum Geology, 110, 287–298. doi: 10.1016/j.marpetgeo.2019.07.028.

Wu GG, Chen ZR, Zhang AS, Zhou J, Hou YN, Xie X, Wu JS, Kong XW, Li S. 2023. Experimental studies on the performance evaluation of water-soluble polymers used as temporary plugging agents. Frontiers in Physics, 11, 1174268. doi: 10.3389/fphy.2023.1174268.

Yang J, Li L, Song Y, Tong G, Zhang MH, Zhang H. 2023. Current status and prospects of offshore oil and gas drilling technology development in China. Acta Petrolei Sinica, 44(12), 2308–2318 (in Chinese with English abstract). doi: 10.7623/syxb202312019.

Yang MJ, Chong ZR, Zheng JA, Song YC, Linga P. 2017. Advances in nuclear magnetic resonance (NMR) techniques for the investigation of clathrate hydrates. Renewable and Sustainable Energy Reviews, 74, 1346–1360. doi: 10.1016/j.rser.2016.11.161.

Ye JL, Wei JG, Liang JQ, Lu JG, Lu HL, Zhang W. 2019. Complex gas hydrate system in a gas chimney, South China Sea. Marine and Petroleum Geology, 104, 29–39. doi: 10.1016/j.marpetgeo.2019.03.023.

Ye L, Qiu ZS, Chen XH, Zhong HY, Zhao X, Bao D. 2020. Evaluation on the ability of a new self-degrading lost circulation agent to plug fractures and protect reservoirs. Drilling Fluid & Completion Fluid, 37(6), 731–736 (in Chinese with English abstract). doi: 10.3969/j.issn.1001-5620.2020.06.009.

Zarrintaj P, Jouyandeh M, Ganjali MR, Hadavand BS, Mozafari M, Sheiko SS, Vatankhah-Varnoosfaderani M, Gutiérrez TJ, Saeb MR. 2019. Thermo-sensitive polymers in medicine: A review. European Polymer Journal, 117, 402–423. doi: 10.1016/j.eurpolymj.2019.05.024.

Zhao K, Liu L, Liao B, Wang JT, Chen LQ, Sun JS. 2024. Numerical simulation analysis of multi-physics field coupling in deepwater gas hydrate reservoir drilling. Shipbuilding of China, 65(3), 175–186 (in Chinese with English abstract). doi: 10.3969/j.issn.1000-4882.2024.03.016.

Zhao K, Wang JT, Liao B, Cai WH, Liu L, Sun JS. 2025. Simulation and analysis of wellbore stability for drilling wells in deep and complex formations. Thermal Science, 29(Part B), 1515–1519. doi: 10.2298/tsci2502515z.

Zhao YC, Zhang YY, Huang MX, Mao XK. 2023. Application of low field nuclear magnetic resonance in the experimental study of natural gas hydrate. Laboratory Science, 26(3), 64–68 (in Chinese with English abstract). doi: 10.3969/j.issn.1672-4305.2023.03.017.

Zhu BW, He ZJ, Jiang GS, Ning FL. 2024a. Molecular design of switchable nanochannels modified by zwitterion polymer chains with dissipative particle dynamics simulation. Polymer, 290, 126602. doi: 10.1016/j.polymer.2023.126602.

Zhu BW, He ZJ, Jiang GS, Ning FL. 2024b. Transport properties of aqueous methane solutions and blocking behavior of intelligent-responsive temporary plugging agent in a switchable nano-channel: A dissipative particle dynamics simulation study. Macromolecular Rapid Communications, 45(21), 2400388. doi: 10.1002/marc.202400388.

Zhu YH, Wang PK, Pang SJ, Zhang S, Xiao R. 2021. A review of the resource and test production of natural gas hydrates in China. Energy & Fuels, 35(11), 9137–9150. doi: 10.1021/acs.energyfuels.1c00485.